Revista Virtual de Química

Article

http://dx.doi.org/10.21577/1984-6835.20240073

Prominent Methods to Process, Characterize and Organize Starch Polymers

Métodos Especiais para Processar, Caracterizar e Organizar Polímeros do Amido

*Marinara Andreola,[a] Daiani C. Leite,[b] Andresa da C. Ribeiro,[c] Roberta Zucatti,[a] Andrielle Vailatti,[a] Diana A. de Sousa,[a] Luís P. Fonseca,[d] Nádya P. da Silveira[a,]**

[a] Universidade Federal do Rio Grande do Sul, Instituto de Química, Programa de Pós-Graduação em Química (PPGQ), Zip Code 91501-970, Porto Alegre-RS, Brazil
[b] Universidade Federal de Santa Maria, Departamento de Física, Laboratório de Superfícies e Macromoléculas, Zip Code 97105-900, Santa Maria-RS, Brazil
[c] Instituto Federal de Educação, Ciência e Tecnologia Sul-riograndense, Campus Charqueadas, Zip Code 96745-000, Charqueadas-RS, Brazil
[d] Universidade de Lisboa, Instituto Superior Técnico, Instituto de Bioengenharia e Biociências, Departamento de Bioengenharia, Zip Code 1049-001, Lisboa, Portugal

E-mail: nadya@iq.ufrgs.br

Submissão: 17 de Setembro de 2024

Aceite: 17 de Dezembro de 2024

Publicado online: 16 de Janeiro de 2025

Starch is the most abundant storage reserve carbohydrate in different plants such as seeds, fruits, tubers, and roots. This carbohydrate is a renewable raw material and can be used for many pharmaceutical, cosmetic, food, and industrial applications. In the last decade, several groups have been dedicated to studying starches, applying enzymatic and chemical modification of the granules, improving their properties, and developing new materials with specific features. In this work, we describe some research done in our group on starch and its polymers over the years, using several unconventional ways to process, characterize, and organize them. We explored starch hydrolysis under different conditions and characterized the crystallization degree, gelatinization temperature, and morphology. Besides that, different light scattering techniques were used to study amylose fractions extracted from starch. Also, acetylated amylose was applied to prepare amylose-based inclusion bromothymol blue complexes. Finally, starch nanoparticles were fabricated, showing a change in the intern organization pattern. All those key findings support the research carried out by the group over time and give new challenges and opportunities to explore starch and its polymers.

Keywords: Starch polymers; acetylated amylose; amylose-bromothymol blue complexes; starch nanoparticles.

1. Introduction

Starch is arranged as semi-crystalline granules composed of two homopolymers of α-D-glucose (amylose and amylopectin) containing crystalline and amorphous areas.[1] The possibility of modifying their granules and improving the specific characteristics such as size, porosity, and crystallinity increases the search for new methodologies and applications.[2-4] Starch polymers are one of the most abundant and renewable sources of carbohydrates, and besides this, they are safe and inexpensive.[5,6] Starch polymers' auto-organization and complexation ability have been studied as the key to preparing a new natural-based system.[7,8]

Many studies highlight the growing importance of starch and starch polymers in producing new mesoscopic colloids.[9-19] However, starch granules are limited by their specific physical properties, such as insolubility in cold water, granule size, and amylose/amylopectin content.[20-21] To overcome these limitations, some physical or chemical modifications can be applied.[22-24] For instance, boiling water can help the gelatinization process.[25-27]

Regarding the modification in morphology, the chemical treatment of starch performed under acid conditions, including the application of an external electric field, can increase the crystallinity of starches. At the same time, the gelatinization temperature range also increases.[12] Another possibility is the enzymatic treatment of starch granules using α-amylase and amyloglucosidase, which gives hierarchical porosities inside the granules.[9,10] Ultrasound treatment can reduce the molecular weight of starch polymers, which reduces solution viscosity and, under appropriate conditions, decreases the polydispersity and hydrodynamic and gyration radius.[13,28]

Amylose and amylopectin can be extracted from starch by dissolving in aqueous solution, and amylose can be chemically modified using acetylation to increase its hydrophobicity, which may be applied as hydrophobic guest molecules.[11-14,29] Furthermore, starch polymers can be physically reorganized into nanodomains and rearranged as stable nanostructures, usually called starch nanoparticles.[16,30,31]

Regarding the several possibilities to rearrange and organize starch and starch polymers, in this work we intend to present results, which are exploring some aspects less known of autoorganized systems obtained with starch and starch polymers. The main results are exploring

-ray diffraction (XRD), small-angle X-ray scattering (SAXS), polarized and depolarized light scattering (DLS and SLS), UV spectroscopy (UV-Vis), and scanning electron microscopy (SEM), showing the potential of starch as a starting material for many applications.

2. Experimental

2.1. Materials

Dimethyl sulfoxide (DMSO), acetic anhydride, amylose (from potato starch, dried at 50.0 °C for 12 h), commercial amylose, native amylose, and bromothymol blue dye (BB) were purchased by Sigma Aldrich®. Hydrochloric acid (HCl, 37%) was obtained from NEON (São Paulo, Brazil). Potassium hydroxide (KOH) was purchased by Dinamica (São Paulo, Brazil). Thymol was purchased by Vetec (Rio de Janeiro, Brazil). Regular corn starch powder (18% amylose, dried at 40.0 °C for 48 h) and high amylose corn starch (Hylon VII, 52% amylose, dried at 40.0 °C for 48 h) were gently given by Ingredion (São Paulo, Brazil). Amylose from rice starch was also used (BR-IRGA 410 industrial *indica* rice starch, 32% amylose, 58% amylopectin).

2.2. Methods

The following sections present different methods applied to process, characterize and prepare starch granules and their polymers.

2.2.1. Acid hydrolysis of starch granules

Regular corn starch (5%, w/v) dispersed in HCl (1.0 mol L^{-1}) was submitted to different acid hydrolysis times (24, 96, and 168 h) at room temperature (20.0 ± 3.0 °C). After, the samples were centrifuged, washed with distilled water, then dried at 40.0 °C in an oven.

Analysis of hydrolyzed starch samples was performed by X-ray diffraction (XRD) using a D-500 diffractometer (Siemens), operating at 40 kV and 17.5 mA from 2θ = 3° to 40°. XRD patterns data were processed using *OriginPro* 2019 software and smoothed with the *Adjacent Averaging* tool. Crystallinity degree (X_c) was estimated by the method described by Hulleman *et al.*:[32]

$$X_C = \frac{H_C}{(H_C + H_A)} \quad (1)$$

where H_C is the intensity of the crystalline peaks and H_A is the intensity of the amorphous component of the peaks (background).

The birefringence of the starch granules was observed by optical microscopy (Olympus BX41, digital camera DP73, USA) under polarized light. Gelatinization temperature ranges of samples were also measured by optical microscopy under polarized light with temperature control (oven FP82HT, Mettler Toledo and FP90 processor, Mettler Toledo, USA). Samples were dispersed in distilled water (0.025 g mL^{-1}) and observed at a 10.0 °C min^{-1} heating rate, starting at 50.0 °C.

Scanning electron microscopy (SEM) was performed with an EVO MA10 (Zeiss, Germany). Dried samples were sputter-coated with an Au layer before SEM acquisition.

Thermogravimetric analysis (TGA) (TA Instruments) was carried out for dried samples from 30.0 to 450.0 °C, with a heating rate of 10.0 °C min^{-1} under an ultra-pure nitrogen atmosphere at 25 mL min^{-1}.

2.2.2. Amylose isolation

Amylose was isolated from industrial *indica* rice starch (BR-IRGA 410, 32% amylose and 58% amylopectin) by precipitation with thymol.[33] The starch was dispersed in boiling water (1% w/v) and kept under stirring for 30 min. Sodium chloride (0.1% w/v) and thymol (0.13% w/v) were added to the mixture and the solution was rapidly cooled to room temperature. The mixture was allowed to settle for 48 h for the complex precipitation. The precipitate was washed with saturated thymol solution, ethanol and ether. The final product was dried in vacuum at room temperature. Isolated amylose was dispersed in KOH 1 mol L^{-1}, gently stirred overnight, and then diluted till pH 10.5. The sample (5 mL in KOH at pH 10.5) was submitted to a gel filtration chromatography in a column (2.6 x 100 cm) packed with Sephacryl S-400 percolated with KOH pH 10.5 at a flow rate of 8 mL per hour (linear flow 1.5 cm h^{-1}), at 4.0 °C. The initial 5 mL were rejected and the following 1 mL fractions were collected for light scattering analysis.

Also, after complete amylose dissolution in KOH 1 mol L^{-1}, the amylose solutions were diluted with water or KCl solution to obtain different ionic strengths. The samples were filtered (0.22, 0.45, and 1.20 μm pore membranes) and placed into dust-free cells for light scattering experiments. The measurements were performed at different storage times.

The characteristic amylose fraction was assayed by the hydrodynamic radius (R_h) using dynamic light scattering (DLS). The radius of gyration (R_g) was determined by static light scattering (SLS) using the dissymmetry method, as well as the structure-sensitive parameter (ρ), a combination of R_g and R_h. SLS were performed on an automatic BI-200M goniometer and a BI-9000 AT digital correlator (Brookhaven Instruments). A coherent He-Ne laser (λ = 632.8 nm) was used as a light source. All solutions were thermostated in a refractive-index-matching liquid (decaline) at room temperature. The experiments were performed in triplicate. SLS and DLS experiments were performed at 9 different θ scattering angles within the range 35° < θ < 145°. Three individual 3 min runs per angle were taken in DLS experiments.

In SLS, the Zimm method was applied to estimate the molecular weight (M_w).[34] The R_g for the amylose samples

was obtained by SLS using the dissymmetry method,[35] according to the following relation:

$$\frac{I_\theta}{I(180° - \theta)} \cong 1 + 2\left(\frac{R_g}{3}\right)q^2 \quad (2)$$

where q^2 is the square of the scattering vector and I is the intensity of the scattered light.

In DLS analysis, the fluctuations of the scattered intensity are due to the Brownian motion of the macromolecules in a scattering volume. The R_h can be derived from the diffusion coefficient in infinite dilution, D_o, via the Stokes-Einstein relation:

$$R_g = \frac{k_B T}{(6\pi\eta_0 D_0)} \quad (3)$$

where k_B is the Boltzmann constant, T is the absolute temperature of the sample, and η is the viscosity of the medium. If D is determined with $q_{\to 0}$ e $c_{\to 0}$, R_h corresponds to the absolute hydrodynamic radius. In different cases, it is an apparent hydrodynamic radius.

2.2.3. Acetylated amylose and inclusion complexes with bromothymol blue

Acetylated amylose (AA) was prepared according to the method proposed by Mark and Mehltretter[36] with modifications.[11] Amylose from potato starch (M_w > 150,000 g mol^{-1}) was dried at 50.0 °C for 12 h, then 1 g of amylose and 3 mL acetic anhydride were mixed in a glass vial and the solution was stirred on a magnetic stirrer at 500 rpm for 5 min. Right after, 0.9 mL of 50% NaOH aqueous solution was added under continuous stirring for 90 min at 90.0 °C. Then, the suspension was cooled to 50.0 °C and the amylose was precipitated with the addition of 10 mL of 96% ethanol. At once, the solution was centrifuged at 3,000 rpm for 10 min (Labofuge 200, Heraeus Instruments) and then the precipitate was washed with 96% ethanol and centrifuged two times till most acetic anhydride was eliminated. Finally, the precipitate was dried for 12 h in a vacuum pump at 2 × 10^{-2} mbar (rotary vane pump RZ 2.5, Vacuubrand) at 25.0 °C.

Amylose-bromothymol blue (A-BB) inclusion complexes were prepared with 10 mg of amylose dissolved in 20 mL of 0.1 mol L^{-1} KOH solution. The solution was stirred on a magnetic stirrer for 6 h at 90.0 °C under a N_2 atmosphere. A bromothymol solution (0.01 g L^{-1}) was prepared separately by dissolving in 0.1 mol L^{-1} KOH solution for 30 min at 25.0 °C and then added into native amylose (A) solution (1:30 v/v).[37] The inclusion complex of acetylated amylose-bromothymol blue (AA-BB) was prepared according to a similar procedure, except the acetylated amylose was dissolved in water at neutral pH (0.5 g L^{-1}) and then mixed with an aqueous solution of bromothymol blue (0.01 g L^{-1}). Both solutions were mixed and stirred for 24 h at 40.0 °C or 65.0 °C. All experiments were performed in triplicate.

Complex formation between native (A) or acetylated amylose (AA) with bromothymol blue was accessed by UV-Vis spectroscopy. The UV-Vis absorbance spectra were obtained on a PerkinElmer spectrophotometer 554 using a quartz cell with an optical length of 1 cm in water or 0.1 mol L^{-1} KOH. UV-Vis spectroscopy was also used to determine the inclusion efficiency (%IE) and loading capacity (%LC) of bromothymol blue in the inclusion complexes. For this, the absorbance of various bromothymol blue concentrations was recorded over wavelengths ranging from 200-700 nm. The maximum peak, with minimum interference, was centered at 616 nm. For the inclusion complexes, free bromothymol blue concentration was determined in the same manner. From that, the percentage of included bromothymol blue and loading capacity were determined using Eqs. (4) and (5):

$$\%IE = 1 + \frac{\text{Quantity of BB} \in \text{the complex}}{\text{Total quantity of BB}} \times 100 \quad (4)$$

$$\%LC = 1 + \frac{\text{Quantity of BB} \in \text{the complex}}{\text{Total quantity of amylose}} \times 100 \quad (5)$$

All measurements were carried out at 25.0 ± 0.1 °C. All data shown represent the average of, at least, three independent determinations.

The apparent average hydrodynamic radius (R_h) of inclusion complexes was performed by DLS using a Zetasizer Nano ZS (Malvern Instruments, USA) equipped with a 4 mW He-Ne laser. Measurements were performed at a wavelength of 632.8 nm, using the detection angle of 173°, at 25.0 ± 0.1 °C. All samples were purified through a 0.45 µm filter (PTFE, Millex Millipore) and each sample was measured 3 times. The reported values are the mean diameter ± s.d.

The zeta potential (ZP) was measured by a Malvern Zetasizer (Malvern Instruments, USA) at 25.0 ± 0.1 °C. ZP was calculated using the Smoluchowski equation from the electrophoresis mobility and electric field strength. The value was recorded as the average of five measurements and the values reported are the mean ± s.d.

2.2.4. Starch nanoparticles

A solution containing 2% high amylose corn starch (w/v) in DMSO/H_2O (ratio 9:1) was prepared and maintained under magnetic stirring at 40.0 °C for 2 h. After cooling to room temperature, the solution (viscous and cloudy) was submitted to ultrasonic treatment (Branson Sonifier, model 250 and 450, 20 kHz, USA, DES500 tip) for 1 min, using 100% amplitude. In this step, ultrasound was used to reduce the starch polymers' molecular weight.[13] An ice bath was used around the sonicated sample to prevent heating due to sonication. After, 1 mL of the sonicated solution was added drop by drop in 20 mL of absolute ethanol,[38] under a magnetic stirrer at 900 rpm controlled speed (final concentration of 20 mg mL^{-1}), for 60 min. After this, the

suspension was purified through 3 successive centrifugations (3,000 rpm, 15 min) and re-suspensions in absolute ethanol to remove DMSO and residual water and then dried at 40.0 °C for 24 h.

The starch nanoparticles were characterized by XRD using the same procedure and described in section 2.2.1 and the crystallinity degree (X_c) was estimated using equation 1.

3. Results and Discussion

In the following sections, the main results related to starch granules and their polymers are presented, prepared as described in the previous sections.

3.1. Acid hydrolysis of starch granules

Acid hydrolysis is one of the most common methods applied to starch modification.[39] Our research group performed experiments called free acid hydrolysis (FAH), in which the ions responsible for promoting hydrolysis are free in solution, unlike the hydrolysis methodology of a previous publication, where an external electric field was employed to orientate the ions in solution, and the method was named oriented acid hydrolysis (OAH).[12] The physicochemical properties of modified starches by FAH and OAH are shown in Table 1. The results were obtained by XRD, optical microscopy, TGA, and SEM.

The increase in relative crystallinity (Table 1) until 96 h of FAH is due to the primary degradation of amorphous regions since amylose chains are more susceptible to acid attack and of the lamella containing the branching points in amylopectin too. Depending on hydrolysis time, the acid can also interact with amylopectin clusters, as indicated by the decrease of crystallinity in sample FAH3. Despite changes in the crystallinity degree, all samples kept a characteristic A-type crystalline profile (peaks at 15.0°, 17.0°, 18.0°, and 23.0° 2θ), as can be seen in Figure 1. For the sample OAH3, a similar behavior was detected as compared to the FAHs.[12]

Initially, the acid attacks the granule surface, causing morphological changes. The superficial pores start to function as channels to the interior of the granules with hydrolysis time, allowing the acid to reach regions closer to the hilum.[40] SEM images (Figure 2) showed that, while regular corn starch granules presented smooth surfaces (Figure 2a), the acid-treated samples acquired small cavities at the surface, which are more pronounced as the hydrolysis time increases. Also, according to the hydrolysis time, the surface of granules highlights its polygonal shape (Figure 2b, 2c, 2d). Yan *et al.*[41] reported a similar cavity pattern in nano-precipitated amylose granules submitted to acid hydrolysis.

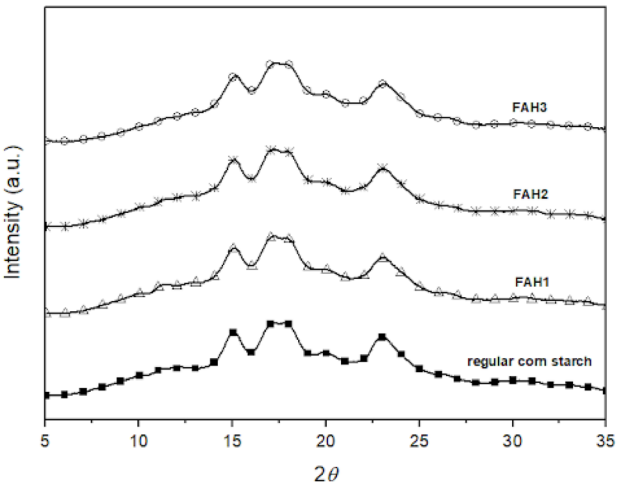

Figure 1. XRD patterns of regular corn starch and acid-treated starch samples prepared by free acid hydrolysis method (FAH)

In searching for improvements in hydrolysis conditions, such as time or effectiveness of the treatment without disrupting the granule, the most common methodology is associating heat with the treatments.[32,42] In previous work, we incorporated a device to upgrade the hydrolysis methodology employing an external electric field.[12] Corn starch was submitted to a fixed voltage, varying the external electric field application time and the number of cycles. The optimal reaction condition was five cycles of 10 seconds each. This method (OAH) allowed the reaction time to be reduced, and the acid attack intensified the surface modifications. This behavior is due to the organization provided for the ions in solution by the applied potential. The

Table 1. Crystallinity degree, thermal degradation temperatures, and gelatinization temperatures of regular corn starch (RCS) and acid-treated starches prepared by free acid hydrolysis (FAH)

Sample	Hydrolysis time / h	Crystallinity degree / %	Thermal degradation temperature / °C	Gelatinization temperature range / °C[a]	ΔT / °C[b]
RCS	-	33.4	316.5	68.8 – 73.0	4.2
FAH1	24	39.7	301.3	56.8 – 69.5	12.7
FAH2	96	48.5	304.4	57.0 – 71.9	14.9
FAH3	168	35.0	304.6	63.8 – 73.6	9.8
OAH3[c]	0.014	54.2	-	64.5 – 75.5	11.0

[a] Onset and offset temperatures are related to the beginning of and the total Maltese cross disappearance, respectively monitored by polarized light optical microscopy. [b] ΔT: gelatinization temperature range. [c] Prepared by oriented acid hydrolysis (OAH) as reference .[12] Thermal degradation temperature was not evaluated.

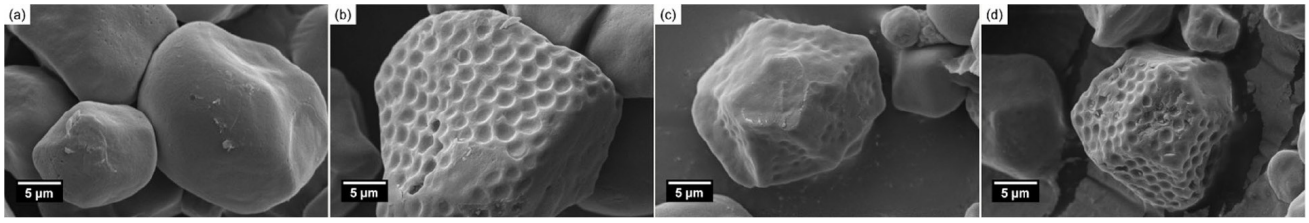

Figure 2. SEM images of (a) regular corn starch; (b) FAH1; (c) FAH2; and (d) FAH3 (scale bar = 5 µm)

acid treatment also affects the internal lamellar organization of the granules, as evaluated by small-angle X-ray scattering (SAXS).[12] The main difference between FAH and OAH can be observed through the corn starch characteristic peak in *q*-value of 0.6 nm^{-1}, as presented at Figure 3, corresponding to the periodic arrangement of the lamellar structure of starch.[43] In our former work,[12] the samples prepared under the influence of oriented acid hydrolysis maintained the characteristic peak with slight changes in intensity and subtle shifts in the peak *q*-values compared with the regular corn starch. Hence, we concluded that the semi-crystalline lamellar structure was maintained. In the sample FAH1, the peak disappeared due to the loss of lamellar organization, corroborating the inner modifications caused by FAH. Glycosidic bonds were broken in the amorphous and crystalline regions of the granules.[44]

The crystalline order of starch granules and their internal lamellar organization are essential in starch properties, such as thermal stability and granular gelatinization profile. The lower onset and offset gelatinization temperatures of acid-treated samples (Table 1) compared to regular corn starch could be related to internal structural changes, including the loss of lamellar organization detected by SAXS, which creates instability and makes the granules less resistant towards gelatinization. The evident increase in the gelatinization temperature range (ΔT) could be interpreted as an effect of longer amylopectin double helices that may form due to the removal of branch points.[45] Another possibility is that it is a consequence of the increase in relative crystallinity since a lower amylose content attenuates the destabilizing effect of swelling in amorphous regions on the melting of the crystallites.[46] It has already been reported in the literature that there is no significant relationship between microstructure (crystallinity and granular size) and the thermal degradation process.[47] Such reports agree with the data in Table 1, in which it can be seen that a significant increase (FAH1 and FAH2) or decrease (FAH3) of the crystallinity degree was not related to any pattern regarding the thermal degradation temperatures. However, the loss of lamellar organization detected in sample FAH1 by SAXS,[12] contributed to a decrease in its thermal degradation temperature compared to regular corn starch (Table 1). The thermal behavior of FAH2 and FAH3 indicates that a loss of lamellar organization may have also occurred in these samples.

3.2. Amylose isolation

It is known that the challenge for the preparation of natural starch polymers is the separation of amylose and

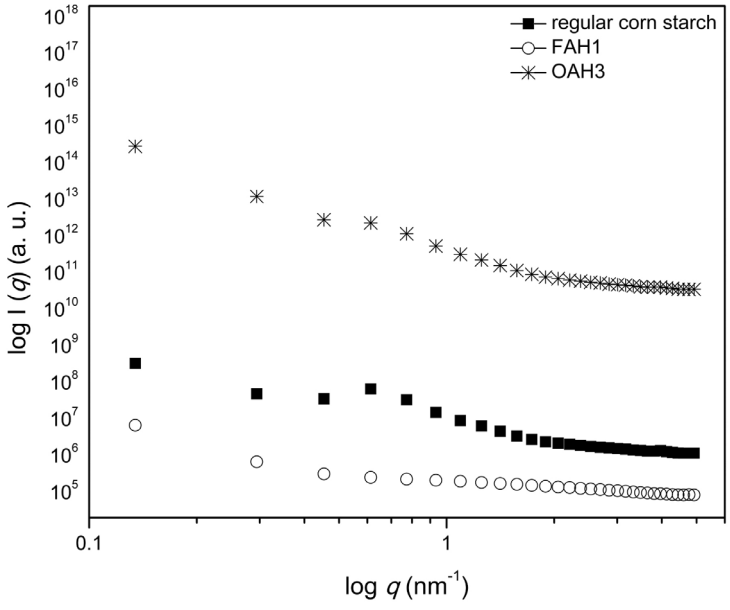

Figure 3. SAXS curves of regular corn starch, free and oriented acid hydrolysis covering all q-range measured

amylopectin.[48-51] In our group, we extracted amylose from industrial *indica* rice starch. After extraction, amylose was submitted to gel filtration chromatography and the fractions were collected and analyzed without previous filtration. Table 2 shows the different amylose fractions in this work. Where the corresponding mL number represents each fraction, for example, f6 is the fraction collected during the elution of the 6th mL.

Table 2. Hydrodynamic radius (R_h), radius of gyration (R_g), structure-sensitive parameter (ρ), and molecular weight (M_w) for the amylose fractions (*f*)

Fraction	R_h (nm)	R_g (nm)	ρ	M_w (g mol^{-1})
***f*6**	120	84	0.70	1.6 x 10^6
***f*8**	73	64	0.86	9.5 x 10^5
***f*11**	53	45	0.84	4.6 x 10^5
***f*13**	54	44	0.82	4.6 x 10^5
***f*16**	52	44	0.84	4.3 x 10^5
***f*18**	40	32	0.80	2.7 x 10^5

As was foreseen, the respective hydrodynamic radius (R_h) values decrease as a function of the fraction (*f*) eluted, since for the first fractions, the highest molecular weights (M_w) are expected to be eluted. The R_g varies characteristically with the structure of the macromolecules. Also, taking the R_g values (32 to 84 nm), the molecular weight was calculated according to equation $\langle R_g^2 \rangle_z = K_v \langle M_w \rangle^v$, where K_v = 2.71 x 10^{-22} m^2 mol g^{-1} and ν = 1.13, in 0.1 mol L^{-1} KOH.[52] The relation between R_g and *M*w is presented in Figure 4, as a function of the elution volumes collected during the gel filtration chromatography. High R_g and *M*w values were essentially observed up to an elution volume of 10 mL. Then, the values remained quasi-constant and, for elution volumes higher than 16 mL, R_g and *M*w decreased to 32 nm and 2.7 x 10^5 g mol^{-1}, respectively.

The combination of R_g and R_h gives the structure-sensitive parameter (ρ),[53] and at 25.0 °C, ρ was found to be between 0.70 and 0.86 (Table 2) for the different amylose fractions. These values approach what is predicted for a homogeneous sphere (0.788),[53] and agree with those obtained by Roger and Colonna[54] for amylose isolated using thymol. These values also agree with the literature data from starch granules dissolved in an alkaline solution.[55]

Commercial amylose (M_w = 1.7 x 10^5 ± 5% g mol^{-1}) was used to prepare standard solutions and follow the amylose chain's behavior in terms of their hydrodynamic and gyration radius. Figure 5 shows this behaviour under the influence of alkaline (KOH) and salt (KCl) media. Light scattering measurements were done in the amylose concentration range of 0.8 - 1.4 mol L^{-1} to KOH and 0.8-2.2 to KCl. The main results showed that storage time is essential in the solution's amylose chain structure. Hence, we determined the structure-sensitive parameter ρ, under the influence of those different solutions. The values of ρ for amylose in KOH and in KCl are depicted in Figure 6.

As seen in Figure 6, the ρ parameter increases with the storage times for all concentrations in KOH, from approximately 1.4 to 3.2. Most of the –OH groups in the anhydrous glucose units are ionized at high pH (12.5); hence, aggregation of amylose chains and paste retrogradation can be avoided.[45,56] The values of ρ for the amylose in KCl also increase with the storage time for all concentrations, obeying the same behavior as in KOH. Bello-Perez *et al*.[55]

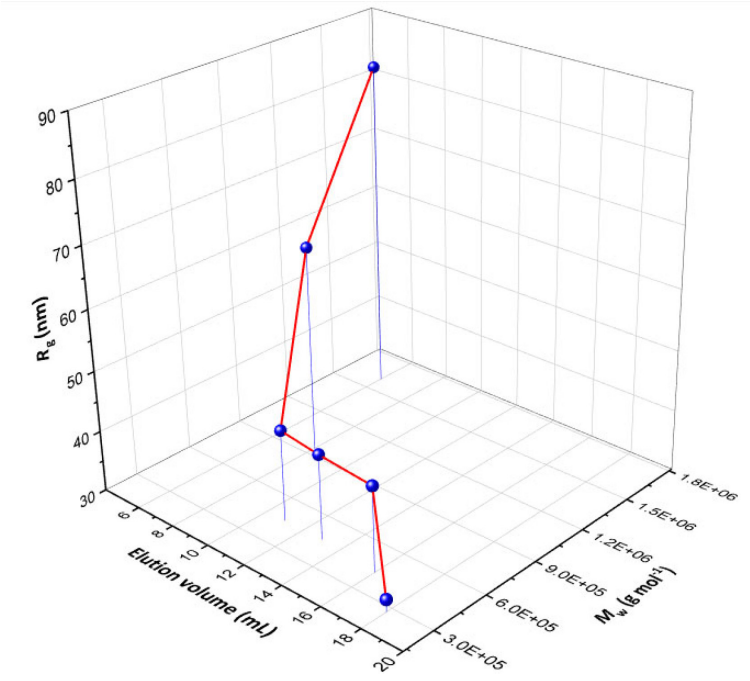

Figure 4. Relationship between the apparent radius of gyration (R_g), elution volume, and molecular weight (Mw) of rice starch amylose

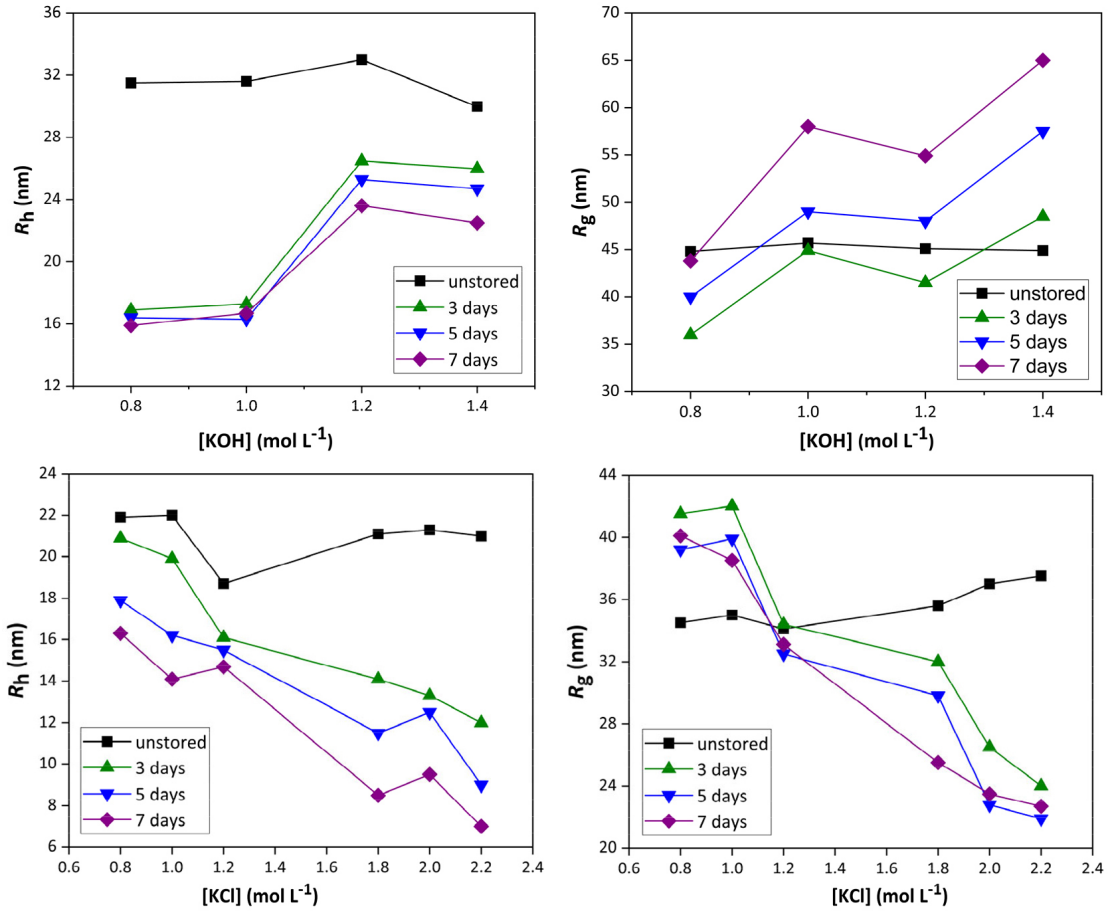

Figure 5. Influence of the KOH (above) and the KCl (below) concentration in the R_h (left) and R_g (right) values of amylose solutions stored for different times. Relative error less than 3%

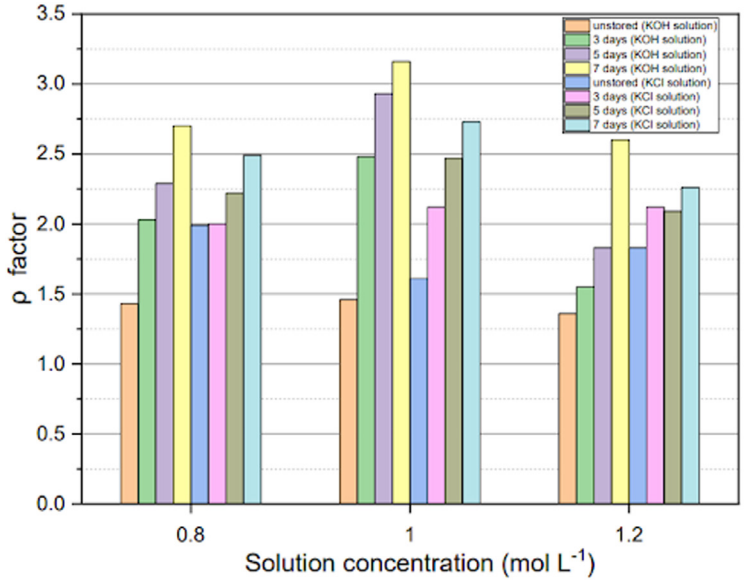

Figure 6. Structure-sensitive parameter, ρ, as a function of the aqueous medium (KOH and KCl) and its concentration and time of storage, at room temperature (20.0 ± 3.0 °C). Relative error less than 5%

reported the same effect for the ρ values during the storage time of amylose in KCl, showing an expected variation in the structure when the storage time increases. As a general rule, KOH is a friendly solvent for amylose and the observed R_g increment when KOH concentration increases can be related to the polymer's good solubility. The

opposite behavior observed in KCl is related to a polymer-polymer interaction preferentially over those of polymer-solvent, through hydrogen bonding and the decrease of the electrostatic repulsion by salt screening effect.[57] An apparent decrease in macromolecular size as a function of salt concentration should be possible because increasing salt content reduces colloidal stability and leads to coagulation. This possibility has been discarded due to the stability of the DLS measurement in the amylose solutions stored for seven days at high salt concentrations, a period in which stability in the diameter of the particles was observed. This high degree of reproducibility in DLS measurements was observed for all samples.

The results point out that amylose does not change its radius instantaneously according to the medium. A delay was verified between amylose stabilization in the alkaline medium and the salt solutions. Interestingly, in 1.2 mol L^{-1} KCl, the effect of storage time was not observed. This KCl solution concentration (1.2 M) stabilizes amylose, and the balance of charges between the amylose and solvent medium is ideal for the amylose coil structure. Based on these results, efforts were devoted to investigating the amylose as a random coil in aqueous solutions, and evidence of amylose coil-to-helix transition in stored dilute solutions was revealed by depolarized light scattering.[58] Following this work, we prepared nanostructures of V-amylose crystalline inclusion compounds with α-naphthol,[59] including a modeling study to solve the molecular structure of the complexes.

3.3. Acetylated amylose and inclusion complexes with bromothymol blue

The use of native amylose (A) is limited because it has low water solubility due to the multiple intramolecular hydrogen bonds between the hydroxyl groups. For this, modification with acetyl groups in the amylose is exciting.[11,60-64] In this modification, the acetyl groups are introduced, preventing the formation of several hydrogen bonds and increasing amylose solubility in water without a significant loss of the helical structure.[11,65,66] Colussi *et al.*[60] studied high-, medium-, and low-amylose rice starches, where the starches were acetylated by using acetic anhydride for 10, 30, and 90 min of reaction. The low-amylose rice starch with 90 min of reaction was more susceptible to acetylation compared to the medium- and high-amylose rice starches. Furthermore, this modification reduced crystallinity, pasting temperature, breakdown, peak and final viscosities, swelling power, and solubility.

Wulff *et al.*[61] investigated five different modified amylose, including acetylated amylose. The amylose was acetylated using acetic anhydride for 15 min at a high pH (at 8 or 9). The authors found that acetylation significantly increased the amount of soluble amylose complexes recovered from aqueous solution and enhanced the inclusion of guest molecules. The method proposed in our group for acetylation of amylose followed the one by Mark and Mehltretter,[36] with modifications,[11] aiming at an amylose with a lower degree of substitution (0.86 ± 0.01) which corresponds to a substitution of about 22% of total OH groups available per anhydroglucose unit. For this low degree of substitution, the acetylated amylose presents higher solubility (0.5 g L^{-1}) in water at neutral pH than native amylose. Modifications may occur essentially in the outside chains, while the inside chains are not involved in substitution.

In this former study,[11] acetylated amylose was used for the inclusion of the rifampicin drug. As a result, the inclusion efficiency and loading capacity increased after the substitution of hydroxyl groups by acetyl groups in amylose, promoting better interaction with drugs. This suggests that the modified amylose-containing acetyl groups have stronger hydrophobic interactions with the piperazine tail of rifampicin.

Below, we present the results of the TGA of the native amylose (A) and acetylated amylose (AA) to examine the changes in the thermal properties of amylose caused by acetylation. TGA results of native amylose showed a two-stage weight loss, with the first peak corresponding to a loss of water around 60.0 - 100.0 °C and a weight loss of 10% (Figure 7a). Once dehydrated, the native amylose sample was stable up to ~300.0 °C. When heated until 500.0 °C, the thermal decomposition with a weight loss of

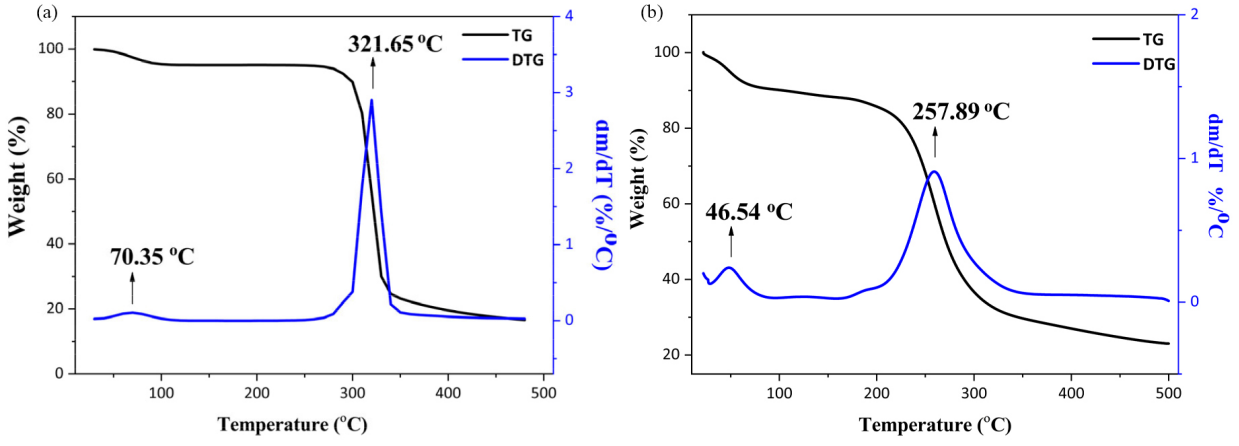

Figure 7. (a) TG/DTG curves of native and (b) acetylated amylose

83% is observed. Acetylated amylose also showed two-stage weight loss (Figure 7b), but the temperature of each event was smaller when compared to the native sample (~ 50.0 °C for 1st stage and ~ 220.0 °C for 2nd stage).

The acetylation promotes partial hydrolysis, reducing the length of the chains of α-D-glucose. This modification promotes more inter-chain space, increasing the heat transfer process and reducing the onset decomposition temperature.[67] Differential thermogravimetric (DTG) results showed that the native amylose samples presented higher decomposition temperatures than acetylated samples, 321.65 °C and 257.89 °C, respectively. According to the literature, the acetylated samples are thermally more stable than native,[67,68] due to the low amount of remaining hydroxyl groups in amylose chains after modification, increased molecular weight, and acetylation covalent binding.

Extending our previous work about inclusion complexes between A and AA with guest molecules, such as the one carried out with rifampicin,[11] we explored the potential of these structures to form inclusion complexes with bromothymol blue dye (BB). BB is a non-metabolized anionic dye,[69] whose deprotonation (pKa ≈ 7.1) opens a sulfone ring, allowing the compound to establish a more extended delocalized electron system that corresponds to a color change from yellow (lower pH) to blue (higher pH) and green at neutral pH (bathochromic shift).[70] This dye was chosen as a model drug because its structure is similar to aspirin, lidocaine, and propranolol.[71] As a result, BB solubilized in aqueous 0.1 M KOH and ultrapure water presented a maximum UV-Vis peak with minimum interference centered at 616 nm (n → π* transition) and 430 nm (π → π* transition), respectively, as shown in Figure 8. After complexation with native amylose (A-BB) and acetylated amylose (AA-BB), the maximum absorption intensities of BB in both solvents decreased. This fact is due to the partial protection of the excitable electrons and chromophores in the amylose cavity, indicating that the inclusion complexes were formed.

Another information obtained through UV-Vis analysis is the inclusion efficiency (% IE) and loading capacity (% LC) of the dye in both of the complexes. The BB inclusion efficiencies were high in both complexes and both temperatures, as presented in Table 3.

These results allow us to conclude that BB molecules can be encapsulated in a hydrophobic environment. However, no difference in inclusion efficiency was found comparing amylose or acetylated amylose BB complexes. According to the literature,[72] the attractive force between the hydrophobic surface and the hydrophobic groups (i.e., benzene rings and $-CH_3$) of the BB molecule is larger than the solvation force between water and BB hydrophilic groups such as $-SO_3$, -Br, and -OH.

For the loading capacity, complexes prepared with amylose in 0.1 mol L^{-1} KOH showed the best results in both temperatures (~ 9.8%). KOH solution is a suitable solvent for amylose, leading to a strong solvation.[73] Then, this result is probably due to the better solubility of A and BB in the KOH solution than that of AA. Besides, amylose

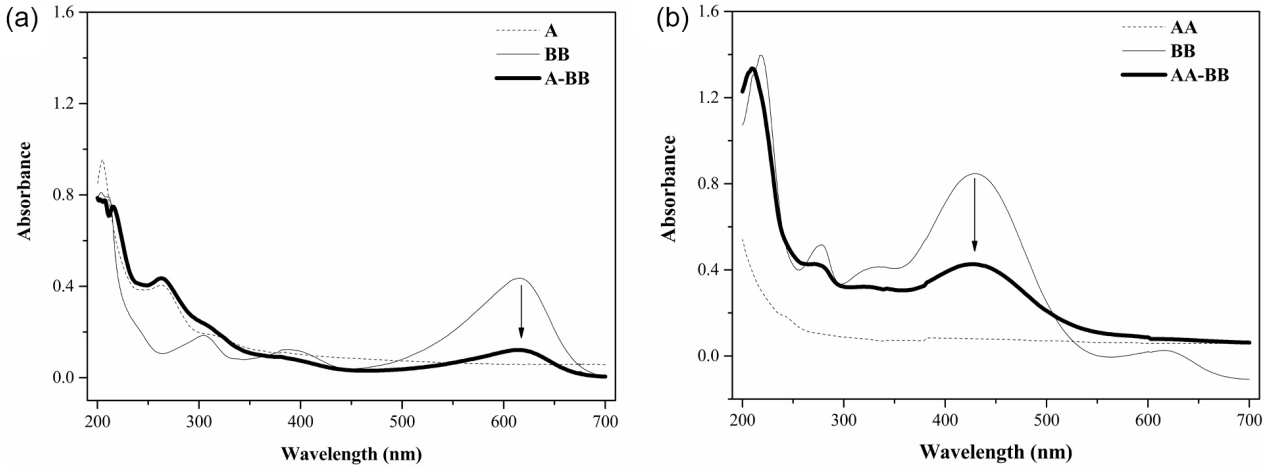

Figure 8. UV-Vis spectrum of samples. In (a), native amylose (A, dotted line), bromothymol blue (BB, black line) and amylose-bromothymol blue (A-BB, bold black line) in 0.1 KOH solution; in (b), acetylated amylose (AA, dotted line), bromothymol blue (BB, black line) and acetylated amylose-bromothymol blue (AA-BB, bold black line) in ultrapure water. The arrow indicates the decrease in absorbance caused by BB inclusion in the amylose or acetylated amylose cavity

Table 3. Inclusion efficiency (% IE) and loading capacity (% LC) of bromothymol blue complexation with amylose or acetylated amylose

	% IE		% LC	
	40.0 °C	**65.0 °C**	**40.0 °C**	**65.0 °C**
Amylose-bromothymol blue	94.10 ± 2.70	90.10 ± 2.10	9.88 ± 0.30	9.80 ± 0.20
Acetylated amylose-bromothymol blue	93.70 ± 0.40	92.90 ± 0.20	1.37 ± 0.20	1.29 ± 0.10

has OH- groups that can promote a nucleophilic attack in BB, shifting the indicator into a colorless form. However, in this case, despite the increase in the loading capacity, the decrease in color is not evident. In this case, the AA molecule presents a low degree of substitution (0.86 ± 0.01).[11] Thus, as the amount of OH- ions is decreased, this attack's action is also decreased.

DLS characterization showed that the A-BB complex displays a higher hydrodynamic particle size (~ 113.0 nm) than the AA-BB complex (~ 76.0 nm). The BB chains are probably surface-exposed and oriented toward the solvent for the complex prepared with A. This hypothesis is in remarkable agreement with the result of a study about the formation of amylose inclusion complexes.[74] For the complex prepared with AA, the size of the complex is very similar to the A. In this case, it is believed that there is a slight decrease in the helicity of amylose molecules after acetylation. This fact changes the exposed functional groups of AA-BB and decreases the interaction of the guest molecule with the amylose cavity. ZP results indicated electrostatic stability for the A-BB complex with a –47.0 ± 1.0 mV value. This result was already expected because the native amylose molecules present hydroxyl groups on the surface of the complex. The AA-BB complex presented a value of ZP of –6.0 ± 2.0 mV because AA presented a lower amount of hydroxyl groups and had a poorly ionized surface at neutral pH.

Hence, including the BB improved the colloidal stability of the complexes prepared with both samples. This study may provide helpful information about AA and the development of amylose inclusion complexes with similar ligands to BB in pharmaceutical applications, especially in an aqueous environment. Moreover, it is possible to conclude that the acetylation method proposed by our group presents a fast, simple, solvent-free, and low-cost methodology and can be used as a model in other studies about starch and its components.

3.4. Starch nanoparticles

In searching for time-saving and eco-friendly starch nanoparticle preparation, recent literature has been quite innovative, as described by Qiu *et al.*[75] in a review of green techniques for SNP preparation. The authors cite techniques described in the previous section, such as acid hydrolysis. As recent advances, nanoprecipitation, high-pressure homogenization, self-assembly, and mini emulsion crosslinking are reported. In addition to the preparation methodology, the native starch source is also a critical impact factor on the final morphology of the SNPs since different arrangements of the amylopectin double helices induce the formation of different structures. Recently, a review by Troncoso *et al.*[76] reported the use of starch extracted from conventional and non-conventional botanical sources and different nanoparticle synthesis methods, in addition to addressing its use in developing novel drug delivery systems. Sago palm, banana, jackfruit, jack bean, and pea starch are among the non-conventional starch sources reported by the authors.

Two strategies to prepare SNPs can be used, known as bottom-up and top-down. In the first one, glucose molecules and oligomers are self-organized until the formation of nanoparticles. The second strategy includes chemical or physical methods to reduce starch granules or gelatinized starch until nanoscale and nanoparticle formation from long polymeric chains by precipitation or crystallization.[30,77]

In our study, a solution of high amylose corn starch solubilized in DMSO/H_2O (9:1 v/v ratio) was prepared. Afterward, the ultrasound treatment and a nanoprecipitation procedure were applied, as described by our previous work.[13] The SNP characterization by DLS showed particles with R_h ~75 nm, as shown in SEM images (Figure 9).[15]

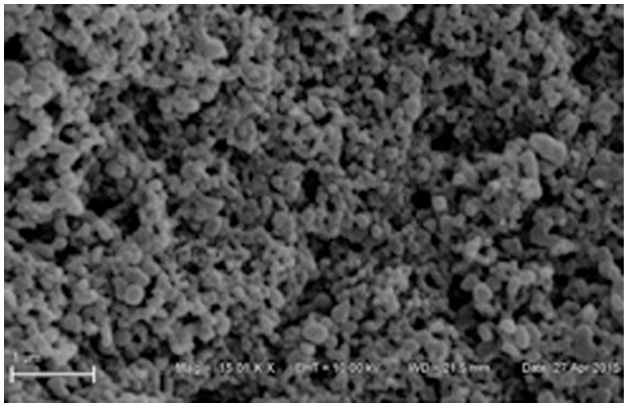

Figure 9. Starch nanoparticles at solid state seen by SEM analysis (scale bar: 1 μm)

Furthermore, analyses of such SNPs using XRD show an effect of recrystallization during nanoparticle formation. Native corn starch and SNPs XRD results presented different scattering patterns, as presented in Figure 10.

According to Figure 10, high amylose corn starch presents a typical profile of A-type crystalline structure, usually found in cereal species.[78] However, the SNP scattering pattern shows a mix of B + V-type crystalline structure (at 2θ values of 5.4, 16.7, 21.7, and 23.5). This kind of change was already described in the literature.[79,80] It can be attributed to a mobility increase of crystalline portion in amorphous regions, leading to a molecular rearrangement involving amylose-amylose and amylose-amylopectin interactions.[81] This finding agrees with the literature, where low recrystallization temperatures and long polymeric chains promote a crystalline packing B + V-type.[82] Another hypothesis would be the formation of V-type crystals during recrystallization due to the formation of inclusion complexes between amylose and ethanol molecules, as described by other authors.[83,84] The calculated crystallinity index (X_C %) was 36.5% and 55.3% for native corn starch and SNPs, respectively. Usually, an increase in crystallinity is achieved in starch granules through an acid or enzymatic treatment (as discussed in section 3.1). In the recrystallization process, it is suggested that a break in polymeric chains in amorphous

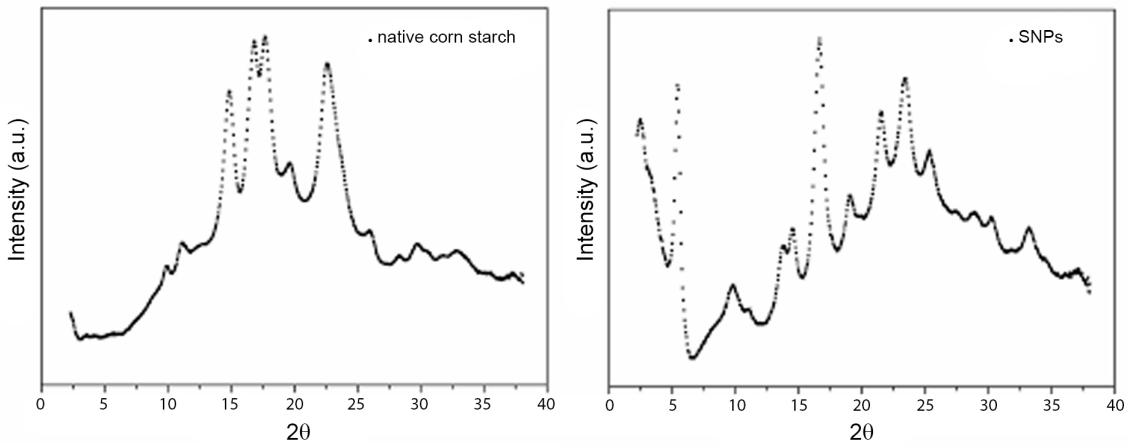

Figure 10. XRD patterns for native corn starch (left) and starch nanoparticles (SNPs) (right)

regions allows for a reorganization of chain segments, resulting in a more crystalline structure.[79,85]

4. Conclusions

It was possible to process, characterize, and organize starch and their polymers in different ways. We presented starch modification, extraction/chemical modification of amylose, and the organization of starch polymers, like inclusion complexes or nanoparticles. The characterization was made by XRD, SAXS, polarized and depolarized light scattering (DLS and SLS), UV-Vis, TGA, and SEM.

The acid hydrolysis of regular corn starch granules showed that this modification in the morphology effectively forms porous in the granules. As presented, all samples kept a characteristic A-type crystalline profile independent of the hydrolysis time. Meanwhile, the use of oriented acid hydrolysis, as discussed, showed a higher crystallinity degree than free acid hydrolysis and a shorter hydrolysis time. Concerning the starch polymers, in this work, we presented that amylose from rice starch was isolated using a precipitation method with a thymol solution. Then, we analyzed the results using gel filtration chromatography, wherein each eluted fraction of amylose showed a decrease in the hydrodynamic radius and molecular weight as expected. Moreover, through the structure-sensitive parameter, we found a homogeneous sphere of amylose. Likewise, the amylose from the starch potato, when chemically modified with acetyl groups, presented a satisfactory result of inclusion efficiency and loading capacity when the inclusion of bromothymol blue was tested, concluding that amylose acetylated can be a reasonable host to other similar compounds. Finally, corn starch was used to produce starch nanoparticles, showing an increase in their crystalline structure, which allowed a rearrangement of the structure of starch polymers.

The results presented above indicated the possibility of using new starch treatments, such as modified acid hydrolysis, and the characterization of systems through structure-sensitive parameters, for example. With this, we were able to reveal starch properties that are little known, as well as other techniques of characterization that have yet to be explored.

Acknowledgments

The authors would like to thank CNPq (grant No. 405662/2016-5) for financial support and the Brazilian Synchrotron facility (LNLS/CNPEM, Proposal 20160060) for SAXS beam time. R. Z. and A. D. V. thank PROPESQ-UFRGS and CNPq for undergraduate fellowships. This study was financed in part by the Coordenação de Aperfeiçoamento de Pessoal de Nível Superior – Brasil (CAPES) – Finance Code 001. We also would like to thank Mateus Borba Cardoso (LNLS/CNPEM) for scientific discussions, and INCT Polissacarideos for support.

Author Contributions

Conceptualization, Nádya P. da Silveira; writing - original draft preparation, Andresa da C. Ribeiro, Daiani C. Leite, Diana A. de Sousa, Marinara Andreola and Nádya P. da Silveira; writing review and editing, Andresa da C. Ribeiro, Daiani C. Leite, Luís P. Fonseca, and Nádya P. da Silveira; supervision, Luís P. Fonseca and Nádya P. da Silveira; project administration, Nádya P. da Silveira; funding acquisition, Luís P. Fonseca and Nádya P. da Silveira. All authors have read and agreed to the published version of the manuscript.

Bibliographic References

1. Vamadevan, V.; Bertoft, E.; Structure-function relationships of starch components. *Starch-Stärke* **2014**, *67*, 55. [Crossref]
2. Bangar, S. P; Ashogbon, A. O.; Singh, A.; Chaudhary, V.; Whiteside, W. S.; Enzymatic modification of starch: A green

approach for starch applications. *Carbohydrate Polymers* **2022**, *287*, 119265. [Crossref]

3. Volant, C.; Gilet, A.; Beddiaf, F.; Collinet-Fressancourt, M.; Falourd, X.; Descamps, N.; Wiatz, V.; Bricout, H.; Tilloy, S.; Monflier, E.; Quettier, C.; Mazzah, A.; Rolland-Sabaté, A.; Multiscale Structure of Starches Grafted with Hydrophobic Groups: A New Analytical Strategy. *Molecules* **2020**, *25*, 2827. [Crossref]
4. Adewale, P.; Yancheshmeh, M. S.; Lam, E.; Starch modification for non-food, industrial applications: Market intelligence and critical review. *Carbohydrate Polymers* **2022**, *291*, 119590. [Crossref]
5. Liang, R.; Jiang, Y.; Yokoyama, W.; Yang, C.; Cao, G.; Zhong, F.; Preparation of Pickering emulsions with short, medium and long chain triacylglycerols stabilized by starch nanocrystals and their in vitro digestion properties. *RSC Advances* **2016**, 6, 99496. [Crossref]
6. Jiang, F.; Feng J.; Hu, W.; Ren, Y.; Ma, C.; Chang, L.; Liu, Y.; Lv, X.; Yu, X.; Du, S-K.; Effects of morphology and rheology of starch nanoparticles prepared from various coarse cereals on emulsifying ability. *Carbohydrate Polymers* **2022**, *298*, 120137. [Crossref]
7. Li, P.; Kierulf, A.; Whaley, J.; Smoot, J.; Herrera, M. P.; Abbaspourrad, A.; Modulating Functionality of Starch-Based Patchy Particles by Manipulating Architecture and Environmental Factors. *ACS Applied Materials & Interfaces* **2022**, *14*, 39497. [Crossref]
8. Parra, A. P.; Ramírez, J. A. M.; Huertas, C. E. M.; Preparation and characterization of native starch-ibuprofen molecular inclusion complexes. *Journal of Drug Delivery Science and Technology* **2021**, *63*,102509. [Crossref]
9. Lacerda, L. D.; Leite, D. C.; Soares, R. M. D.; da Silveira, N. P.; Effects of alpha-Amylase, Amyloglucosidase, and Their Mixture on Hierarchical Porosity of Rice Starch. *Starch-Stärke* **2018**, *70*, 1800008. [Crossref]
10. Lacerda, L. D.; Leite, D. C.; da Silveira, N. P.; Relationships between enzymatic hydrolysis conditions and properties of rice porous starches. *Journal of Cereal Science* **2019**, *89*, 102819. [Crossref]
11. Ribeiro, A. C.; Rocha, A.; Soares, R. M. D.; Fonseca, L. P.; da Silveira, N. P.; Synthesis and characterization of acetylated amylose and development of inclusion complexes with rifampicin. *Carbohydrate Polymers* **2017**, *157*, 267. [Crossref]
12. da Silveira, N. P.; Zucatti, R.; Vailatti, A. D.; Leite, D. C.; Acid Hydrolysis of Regular Corn Starch under External Electric Field. *Journal of the Brazilian Chemical Society* **2019**, *30*, 2567. [Crossref]
13. Peres, G. L.; Leite, D. C.; da Silveira, N. P.; Ultrasound effect on molecular weight reduction of amylopectin. *Starch-Stärke* **2015**, *67*, 407. [Crossref]
14. Peres, G. L.; Leite, D. C.; da Silveira, N. P.; Study of complexes formation between transition metal ions and amylopectin in DMSO/H2O solution. *Starch-Stärke* **2016**, *68*, 1129. [Crossref]
15. Leite, D. C.; Kakorin, S.; Hertle, Y.; Hellweg, T.; da Silveira, N. P.; Smart Starch-Poly(N-isopropyl acrylamide) Hybrid Microgels: Synthesis, Structure, and Swelling Behavior. *Langmuir* **2018**, *34*, 10943. [Crossref]
16. Gutiérrez, G. Morán, D.; Marefati, A.; Purhagen, J.; Rayner, M.; Matos, M.; Synthesis of controlled size starch nanoparticles (SNPs). *Carbohydrate Polymers* **2020**, *250*, 116938. [Crossref]
17. Ahmad, M.; Gani, A.; Masoodi, F. A.; Rizvi, S. H.; Influence of ball milling on the production of starch nanoparticles and its effect on structural, thermal and functional properties. *International Journal of Biological Macromolecules* **2020**, *151*, 85. [Crossref]
18. Ruan, S.; Tang, J.; Qin, Y.; Wang, J.; Yan, T.; Zhou, J.; Gao, D.; Xu, E.; Liu, D.; Mechanical force-induced dispersion of starch nanoparticles and nanoemulsion: Size control, dispersion behaviour, and emulsified stability. *Carbohydrate Polymers* **2022**, *275*, 118711. [Crossref]
19. Morán, D.; Gutiérrez, G.; Mendoza, R.; Rayner, M.; López-Blanco, C.; Matos, M.; Synthesis of controlled-size starch nanoparticles and superparamagnetic starch nanocomposites by microemulsion method. *Carbohydrate Polymers* **2023**, *299*, 120223. [Crossref]
20. Singh, N.; Singh, J.; Kaur, L.; Sodhi, N. S.; Gill, B. S.; Morphological, thermal and rheological properties of starches from different botanical sources. *Food Chemistry* **2003**, *81*, 219. [Crossref]
21. Alcázar-Alay, S. C.; Meireles, M. A. A.; Physicochemical properties, modifications and applications of starches from different botanical sources. *Food Science and Technology* **2015**, *35*, 215. [Crossref]
22. Hoover, R.; The Impact of Heat-Moisture Treatment on Molecular Structures and Properties of Starches Isolated from Different Botanical Sources. *Critical Reviews in Food Science and Nutrition* **2010**, *50*, 835. [Crossref]
23. Yan, H.; Zhengbiao, G. U.; Morphology of modified starches prepared by different methods. *Food Research International* **2010**, *43*, 767. [Crossref]
24. Ashogbon, A. O.; Akintayo, E. T.; Recent trend in the physical and chemical modification of starches from different botanical sources: A review. *Starch-Stärke* **2013**, *66*, 41. [Crossref]
25. Choi, S-G.; Kerr, W. L.; Swelling Characteristics of Native and Chemically Modified Wheat Starches as a Function of Heating Temperature and Time. *Starch-Stärke* **2004**, *56*, 181. [Crossref]
26. Singh, J. ; Kaur, L.; McCarthy, O. J.; Factors influencing the physico-chemical, morphological, thermal and rheological properties of some chemically modified starches for food applications - A review. *Food Hydrocolloids* **2007**, *21*, 1. [Crossref]
27. Wang, S.; Li, C.; Yu, J.; Copeland, L.; Wang, S.; Phase transition and swelling behaviour of different starch granules over a wide range of water content. *LWT - Food Science and Technology* **2014**, *59*, 597. [Crossref]
28. Zhu, F.; Impact of ultrasound on structure, physicochemical properties, modifications, and applications of starch. *Trends in Food Science & Technology* **2015**, *43*, 1. [Crossref]
29. Tang, H.; Fan, S.; Li, Y.; Dong, S.; Amylose: Acetylation, Optimization, and Characterization. *Journal of Food Science* **2019**, *84*, 738. [Crossref]

30. Le Corre, D.; Bras, J.; Dufresne, A.; Starch Nanoparticles: A Review. *Biomacromolecules* **2010**, *11*, 1139. [Crossref]
31. Marta, H.; Rizki, D. I.; Mardawati, E.; Djali, M.; Mohammad, M.; Cahyana, Y.; Starch Nanoparticles: Preparation, Properties and Applications. *Polymers* **2023**, *15*, 1167. [Crossref]
32. Hulleman, S. H. D.; Kalisvaart, M. G.; Janssen, F. H. P.; Feil, H.; Vliegenthart, J. F. G.; Origins of B-type crystallinity in glycerol-plasticised, compression-molded potato starches. *Carbohydrate Polymers* **1999**, *39*, 351. [Crossref]
33. Haworth, W. N.; Peat, S.; Sagrott, P. E.; A New Method for the Separation of the Amylose and Amylopectin Components of Starch. *Nature* **1946**, *157*, 19. [Crossref]
34. Berne, B. J.; Percora, R.; *Dynamic Light Scattering*, 1a. ed., John Wiley & Sons, INC: New York, 1976.
35. Hellweg, T.; Eimer, W. The micro-structures formed by Ni2+-AOT/cyclohexane/water microemulsions: a light scattering study. *Colloids and Surfaces A: Physicochemical and Engineering Aspects* **1998**, *136*, 97. [Crossref]
36. Mark, A. M.; Mehltretter, C. L.; Facile Preparation of Starch Triacetates. *die Stärke* **1972**, *24*, 73. [Crossref]
37. Cohen, R.; Orlova, Y.; Kovalev, M.; Ungar, Y.; Shimoni, E.; Structural and functional properties of amylose complexes with genistein. *Journal of Agriculture and Food Chemistry* **2008**, *56*, 4212. [Crossref]
38. Chin, S. F.; Azman, A.; Pang, S. C.; Size Controlled Synthesis of Starch Nanoparticles by a Microemulsion Method. *Journal of Nanomaterials* **2014**, *299*, 120223. [Crossref]
39. Pratiwi, M.; Faridah, D. N.; Lioe, H. N.; Structural changes to starch after acid hydrolysis, debranching, autoclaving-cooling cycles, and heat moisture treatment (HMT): A review. *Starch-Stärke* **2018**, *70*, 13. [Crossref]
40. Chen, P.; Xie, F. W.; Zhao, L.; Qiao, Q.; Liu, X. X.; Effect of acid hydrolysis on the multi-scale structure change of starch with different amylose content. *Food Hydrocolloids* **2017**, *69*, 359. [Crossref]
41. Yan, X.; Wei, H.; Kou, L.; Ren, L.; Zhou, J.; Acid hydrolysis of amylose granules and effect of molecular weight on properties of ethanol precipitated amylose nanoparticles. *Carbohydrate Polymers* **2021**, *252*, 117243. [Crossref]
42. Zavareze, E. D.; Dias, A. R. G.; Impact of heat-moisture treatment and annealing in starches A review. *Carbohydrate Polymers* **2011**, *83*, 317. [Crossref]
43. Cardoso, M. B.; Westfahl, H.; On the lamellar width distributions of starch. *Carbohydrate Polymers* **2010**, *81*, 21. [Crossref]
44. Wang, S. J.; Blazek, J.; Gilbert, E.; Copeland, L.; New insights on the mechanism of acid degradation of pea starch. *Carbohydrate Polymers* **2012**, *87*, 1941. [Crossref]
45. Chang, Q.; Zheng, B.; Zhang, Y.; Zeng, H.; A comprehensive review of the factors influencing the formation of retrograded starch. *International Journal of Biological Macromolecules* **2021**, *186*, 163. [Crossref]
46. Wang, S. J.; Copeland, L.; Effect of Acid Hydrolysis on Starch Structure and Functionality: A Review. *Critical Reviews in Food Science and Nutrition* **2015**, *55*, 1079. [Crossref]
47. Guinesi, L. S.; da Roz, A. L.; Corradini, E.; Mattoso, L. H. C.; Teixeira, E. D. M.; Curvelo, A.; Kinetics of thermal degradation applied to starches from different botanical origins by non-isothermal procedures. *Thermochimica Acta* **2006**, *447*, 190. [Crossref]
48. Bienvenido, J. O.; In *Starch: chemistry and technology*. Whistler, R.L.; BeMiller, J.N.; Paschall , E. F. eds., Academic Press: NY, 1984, chapter 16.
49. Matsunaga N., Seib P.A.; Extraction of wheat starch with aqueous sodium hydroxide. *Cereal Chemistry* **1997**, *74*, 851. [Crossref]
50. Puchongkavarin H., Varavinit S., Bergthaller W.; Comparative study of pilot scale rice starch production by an alkaline and an enzymatic process. *Starch/Stärke* **2005**, *57*, 134. [Crossref]
51. Nadiha, M. Z. N.; Fazilah, A.; Bhat, R.; Karim, A. A.; Comparative susceptibilities of sago, potato and corn starches to alkali treatment. *Food Chemistry* **2010**, *121*, 1053. [Crossref]
52. Roger, P.; Bello-Perez, L. A.; Colonna, P.; Contribution of amylose and amylopectin to the light scattering behaviour of starches in aqueous solution. *Polymer* **1999**, *40*, 6897. [Crossref]
53. Burchard, W.; Richtering, W.; In *Relaxation in Polymers*. Pietralla, M., Pechhold, W., eds.: Steinkopff, 1989, chapter 4.
54. Roger, P. and Colonna, P.; Molecular weight distribution of amylose fractions obtained by aqueous leaching of corn starch. *International Journal of Biological Macromolecules* **1996**, *19*, 51. [Crossref]
55. Bello-Perez, L. A.; Roger, P.; Colonna, P.; Paredes-Lopez, O.; Laser light scattering of high amylose and high amylopectin materials, stability in water after microwave dispersion. Carbohydrate *Polymers* **1998**, *37*, 383. [Crossref]
56. Suortti, T.; Gorenstein, M. V.; Roger, P.; Determination of the molecular mass of amylose. *Journal of Chromatography A* **1998**, *828*, 515. [Crossref]
57. Cho, J. Y.; Heuzey, M. C.; Begin, A.; Carreau, P. J.; Viscoelastic properties of chitosan solutions: Effect of concentration and ionic strength. *Journal of Food Engineering* **2006**, *74*, 500. [Crossref]
58. Heineck, M. E.; Cardoso, M. B.; Giacomelli, F. C.; da Silveira, N. P.; Evidences of amylose coil-to-helix transition in stored dilute solutions. *Polymer* **2008**, *49*, 4386. [Crossref]
59. Cardoso, M. B.; Putaux, J. L.; Nishiyama, Y.; Helbert, W.; Hytch, M.; Silveira, N. P.; Chanzy, H.; Single crystals of V-amylose complexed with alpha-naphthol. *Biomacromolecules* **2007**, *8*, 1319. [Crossref]
60. Colussi, R.; Pinto, V. Z.; El Halal, S. L. M.; Vanier, N. L.; Villanova, F. A.; Silva, R. M. E.; Zavareze, E. D.; Dias, A. R. G.; Structural, morphological, and physicochemical properties of acetylated high-, medium-, and low-amylose rice starches. *Carbohydrate Polymers* **2014**, *103*, 405. [Crossref]
61. Wulff, G.; Steinert, A.; Holler, O.; Modification of amylose and investigation of its inclusion behavior. *Carbohydrate Research* **1998**, *307*, 19. [Crossref]
62. Zhou, Y.; Li, X. Y.; Lv, Y. B.; Shi, Y. F.; Zeng, Y.; Li, D. F.; Mu, C. D.; Effect of oxidation level on the inclusion capacity and solution stability of oxidized amylose in aqueous solution. *Carbohydrate Polymers* **2016**, *138*, 41. [Crossref]
63. Tang, H. B.; Fan, S. F.; Li, Y. P.; Dong, S. Q.; Amylose: Acetylation, Optimization, and Characterization. *Journal of Food Science* **2019**, *84*, 738. [Crossref]

64. Tang, P.; Liu, Y. C.; Gao, Y.; Wang, Y.; Zhang, H.; Liu, Y. M.; Wu, D. C.; Molecular simulation, characteristics and mechanism of thermal-responsive acetylated amylose V-type helical complexes. *Journal of Materials Chemistry B* **2021**, *9*, 3389. [Crossref]
65. Luo, M. C.; Zhang, X. Y.; Wu, J.; Zhao, J. M.; Modifications of polysaccharide-based biomaterials under structure-property relationship for biomedical applications. *Carbohydrate Polymers* **2021**, *266*, 19. [Crossref]
66. Zhou, D. P.; Liu, S. W.; Song, H. Y.; Liu, X.; Tang, X. Z.; Preparation and characterization of chemically modified high amylose maize starch-ascorbyl palmitate inclusion complexes in mild reaction condition. *LWT - Food Science and Technology* **2021**, *142*, 7. [Crossref]
67. Colussi, R.; Pinto, V. Z.; El Halal, S. L. M.; Biduski, B.; Prietto, L.; Castilhos, D. D.; Zavareze, E. D.; Dias, A. R. G.; Acetylated rice starches films with different levels of amylose: Mechanical, water vapor barrier, thermal, and biodegradability properties. *Food Chemistry* **2017**, *221*, 1614. [Crossref]
68. Garg, S.; Jana, A. K.; Characterization and evaluation of acylated starch with different acyl groups and degrees of substitution. *Carbohydrate Polymers* **2011**, *83*, 1623. [Crossref]
69. Nguyen, T. D.; Le, H. B.; Dong, T. O.; Pham, T. D.; Determination of Fluoroquinolones in Pharmaceutical Formulations by Extractive Spectrophotometric Methods Using Ion-Pair Complex Formation with Bromothymol Blue. *Journal of Analytical Methods in Chemistry* **2018**, *2018*, 11. [Crossref]
70. Yetisen, A. K.; Moreddu, R.; Seifi, S.; Jiang, N.; Vega, K.; Dong, X. C.; Dong, J.; Butt, H.; Jakobi, M.; Elsner, M.; Koch, A. W.; Dermal Tattoo Biosensors for Colorimetric Metabolite Detection. *Angewandte Chemie-International Editio*n **2019**, *58*, 10506. [Crossref]
71. Takada, K.; Muranishi, S.; Sezaki, H.; Pharmacokinetics of the hepatobiliary transport of bromphenol blue as a model of organic anionic compounds. *Journal of Pharmacokinetics and Biopharmaceutics* **1974**, *2*, 495. [Crossref]
72. Qi, Z. M.; Matsuda, N.; Santos, J.; Itoh, K.; Takatsu, A.; Kato, K.; A study of molecular adsorption of bromothymol blue by optical waveguide spectroscopy. *Langmuir* **2003**, *19*, 214. [Crossref]
73. Yang, L. Q.; Zhang, B. F.; Yi, J. Z.; Liang, J. B.; Liu, Y. L.; Zhang, L. M.; Preparation, characterization, and properties of amylose-ibuprofen inclusion complexes. *Starch-Stärke* **2013**, *65*, 593. [Crossref]
74. Nouri, A.; Khoee, S.; Preparation of amylose-poly(methyl methacrylate) inclusion complex as a smart nanocarrier with switchable surface hydrophilicity. *Carbohydrate Polymers* **2020**, *246*, 10. [Crossref]
75. Qiu, C.; Hu, Y.; Jin, Z. Y.; McClements, D. J.; Qin, Y.; Xu, X. M.; Wang, J. P.; A review of green techniques for the synthesis of size-controlled starch-based nanoparticles and their applications as nanodelivery systems. *Trends in Food Science & Technology* **2019**, *92*, 138. [Crossref]
76. Troncoso, O. P.; Torres, F. G.; Non-conventional starch nanoparticles for drug delivery applications. *Medical Devices & Sensors* **2020**, *3*, e10111. [Crossref]
77. Kim, H.-Y.; Park, S. S.; Lim, S.-T.; Preparation, characterization and utilization of starch nanoparticles. *Colloids and Surfaces B: Biointerfaces* **2015**, *126*, 607. [Crossref]
78. Buléon, A.; Gallant, D. J.; Bouchet, B.; Mouille, G.; d'Hulst, C.; Kossmann, J.; Ball, S.; *Chlamydomonas reinhardtii* as a model microbial system to investigate the biosynthesis of the plant amylopectin crystal. *Plant Physiology* **1997**, *115*, 949. [Pubmed]
79. Duyen, T. T. M.; Hung, P. V.; Morphology, crystalline structure and digestibility of debranched starch nanoparticles varying in average degree of polymerization and fabrication methods. *Carbohydrate Polymers* **2021**, *256*, 9. [Crossref] [Pubmed]
80. Dries, D. M.; Gomand, S. V.; Delcour, J. A.; Goderis, B.; V-type crystal formation in starch by aqueous ethanol treatment: The effect of amylose degree of polymerization. *Food Hydrocolloids* **2016**, *61*, 649. [Crossref]
81. Kiatponglarp, W.; Tongta, S.; Rolland-Sabate, A.; Buleon, A.; Crystallization and chain reorganization of debranched rice starches in relation to resistant starch formation. *Carbohydrate Polymers* **2015**, *122*, 108. [Crossref] [Pubmed]
82. Tian, Y. Q.; Yang, N.; Li, Y.; Xu, X. M.; Zhan, J. L.; Jin, Z. Y.; Potential interaction between beta-cyclodextrin and amylose-lipid complex in retrograded rice starch. *Carbohydrate Polymers* **2010**, *80*, 581. [Crossref]
83. Cheetham, N. W. H.; Tao, L.; Variation in crystalline type with amylose content in maize starch granules: an X-ray powder diffraction study. *Carbohydrate polymers* **1998**, *36*, 277. [Crossref]
84. Rondeau-Mouro, C.; Le Bail, P.; Buléon, A. Structural investigation of amylose complexes with small ligands: inter-or intra-helical associations? *International Journal of Biological Macromolecules* **2004**, *34*, 251. [Crossref] [Pubmed]
85. Putaux, J.-L.; Nishiyama, Y.; Mazeau, K.; Morin, M.; Cardoso, M. B.; Chanzy, H.; Helical Conformation in Crystalline Inclusion Complexes of V-Amylose: A Historical Perspective. *Macromolecular Symposia* **2011**, *303*, 1. [Crossref]